Quantum Cascade Lasers

N. Finger, S. Gianordoli, S. Gianordoli, E. Gornik, L. Hvozdara, W. Schrenk, G.Strasser, J. Ulrich, K. Unterrainer, R. Zobl

Institut für Festkörperelektronik, Technische Universität Wien, Floragasse 7, A-1040 Vienna, Austria

1. Quadrupolar deformed microlasers on GaAs/AlGaAs

(S. Gianordoli, W. Schrenk, L. Hvozdara, G. Strasser, K. Unterrainer, N. Finger, E. Gornik)

Quantum cascade lasers (QCLs) are powerful light sources in the mid infrared, a spectral region interesting for gas sensing and pollution monitoring. Low threshold currents, high working temperatures (165 K for microcylinder lasers) and single mode emission with a side mode suppression ratio better than 20 dB are needed for many applications.

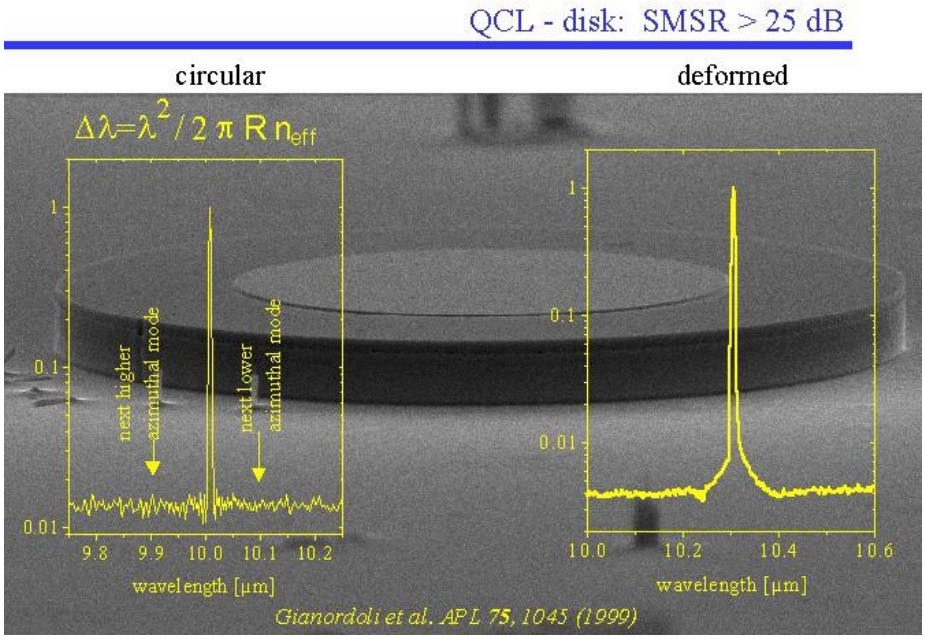

Fig. 1: Single mode spectra of microcavities.

For all driving currents, the described micro-cavity lasers exhibit single mode behavior with a side mode suppression better than 25 dB. No additional side modes are identifiable in the spectra. The positions of the next modes in the emission spectrum of the circular laser (R = 60 μm) are indicated with arrows. The large radius of the deformed micro-laser is R = 50 μm with a deformation coefficient of 0.18. Driving currents are in the range between 200 mA and 2 A, depending on the size of the lasers. Using the following formula in polar coordinates for the radius of the microlasers the so called quadrupolar shaped microlasers shown in Fig. 2 are fabricated using optical lithography and dry etching.

$$r(\phi) = \frac{R}{\sqrt{1+2\varepsilon}}\sqrt{1+2\varepsilon\cos(2\phi)}$$

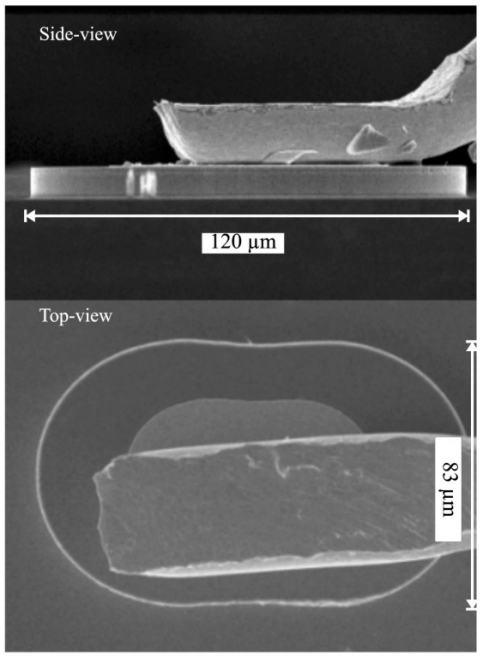

Fig. 2: Top and side view of bonded microcavities.

The side-view and top-view scanning electron pictures of a typical microlaser are depicted in Fig. 2. The etched depth is around 10 µm. For the depicted quadrupolar shaped laser the larger radius has a value R = 60 µm, the smallest value for the radius is 41.7 µm and the deformation is e = 0.22. This results in an active area of 7854 µm^2. For this large deformation the resonator gets concave. In spite of this fact a resonant mode exists and the laser is operating. The distance between the shaped top Au contact and resonator edge is 20 µm. The bonding wire is clearly seen on both views . For a deformation of e = 0.22 the shape of the microlaser rim starts to get concave. This displays excellent quality of the used technology.

2. Self-aligned coupled cavity GaAs/AlGaAs mid-infrared quantum cascade lasers

(L. Hvozdara, G. Strasser, K. Unterrainer, E. Gornik)

Since the introduction of quantum cascade lasers (QCLs) by Faist et al. in 1994 they have undergone a very dynamic development and reached a state of the art among the mid-infrared (MIR) radiation sources. Besides the traditional ridge Fabry-Perot (F-P) geometry, many modifications like distributed feedback-lasers, microcylindrical, quadrupolar as well as disk lasers have been fabricated and characterized.

We present a novel, monolithic, self-aligned focused ion beam cut coupled cavity GaAs/AlGaAs Quantum Cascade Laser emitting in the range of λ = 9.4 µm. Separate pulsing of two optically coupled laser sections enables control of the lasing in single mode regime and in multimode regime. Single mode operation with side mode suppression ratio

better than 25 dB is demonstrated. Mode control over two 3.6 cm^{-1} spaced single modes is shown. Optical output intensity modulation in a range of 20 dB is achieved. The laser exhibits a peak output power in the range of 200 mW at cryogenic conditions.

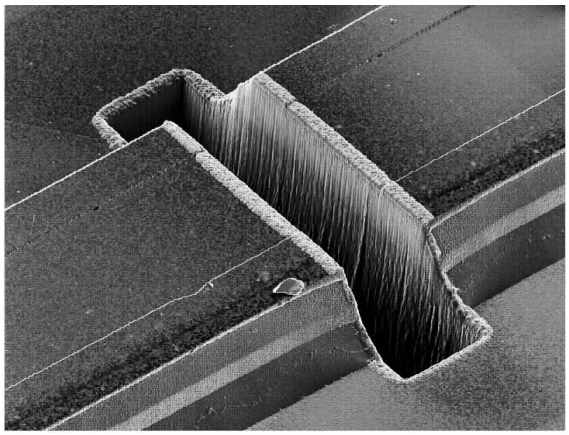

Fig. 3: SEM picture of the FIB processed gap on the $FIBC^3$ laser.

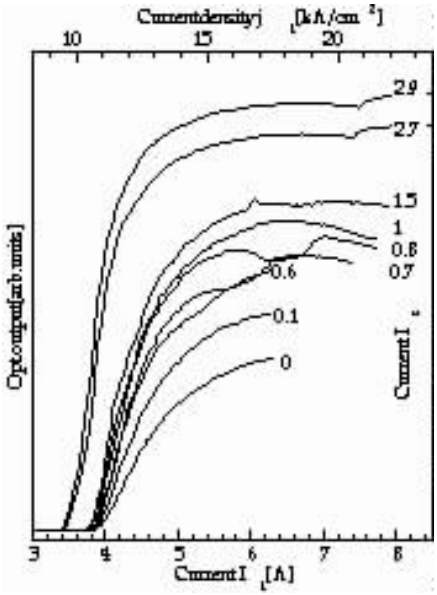

Fig. 4: Optical output vs. current (L-I). The current through the shorter laser section is given as a parameter.

A laser ridge fabricated by common lithographic techniques is modified by trenching a gap perpendicularly across the laser resonator. The extended contact is separated by a shallower trench, in order to enable separate current driving of the two laser sections. The obtained Fib-Cut Coupled Cavity ($FIBC^3$) laser (Fig. 3) is ideally self-aligned, mechanically stable and its fabrication is highly reproducible. This modification converted a two-terminal device into a three terminal device. An independent control of currents through the two sections enables modulation of the output intensity, mode control and single mode operation. Figure 4 shows typical output characteristics (L-I) of a FIBC3 laser with two sections of non-equal lengths. I_L represents the current driven through the

longer section (x-axis) and I_S stands for the current driven through the shorter section (parameter). Variation of I_S from 0 to 2.9 A leads to an increase of the total output intensity by factor of three in the saturation regime. A modulation range of 20 dB in the linear regime has been found. Differential efficiency in the linear regime rises by a factor of 4.1.

3. Development of a terahertz quantum cascade laser

(J. Ulrich, R. Zobl, G. Strasser, K. Unterrainer, E. Gornik)

Quantum cascade lasers are today feasible with vacuum wavelengths up to 17 µm. In order to extend their range into the far infrared, i. e. down to terahertz frequencies, we have designed cascade structures with a level separation of less than the longitudinal optical (LO) phonon energy. Thereby, LO-phonon emission – being the fastest non-radiative scattering channel in the mid-infrared lasers – should be suppressed.

Our emitters are made up of 50 periods of a chirped $Al_{0.15}Ga_{0.85}As/GaAs$ superlattice. Figure 5 displays the conduction band structure. The radiative transition takes place between the first two subbands of a wide quantum well. Multiple ridges were processed for electroluminescence measurements. Using two different spectrometers, a Fourier-transform spectrometer and a magnetically tunable InSb cyclotron resonance detector, we have observed spontaneous emission at 17.3 meV (4.3 THz) with a linewidth of 1.3 meV (see Fig. 6). This is consistent with the calculated energy difference of 17.1 meV. The detected optical power has been roughly estimated from the detector sensitivity to be 10 pW.

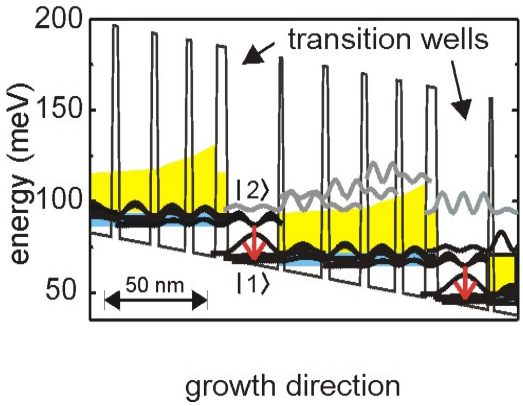

Fig. 5: Conduction band diagram of a terahertz quantum cascade laser.

The main reason for the relatively low power is the low internal quantum efficiency, i.e., the radiative transition rate over the non-radiative rate. The output power could be enhanced by a factor of two by reducing the non-radiative scattering rate in a magnetic field perpendicular to the epitaxial layers. Thereby, the in-plane motion is quantized into Landau levels and electron-electron-scattering is significantly suppressed. The enhancement of the line intensity exhibits characteristic oscillations stemming from resonant tunneling between the two Landau-fans. These results prove directly that the emission from the cascade emitter is limited by fast electron-electron-scattering, which can be controlled by a magnetic field.

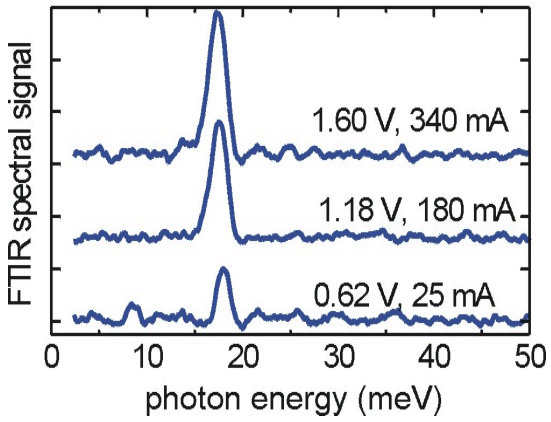

Fig. 6: Emission spectra of a terahertz quantum cascade laser.

4. Distributed Feedback Quantum Cascade Lasers

(W. Schrenk, N. Finger, S. Gianordoli, L. Hvozdara, G. Strasser, E. Gornik)

Quantum cascade lasers are powerful light sources in the mid infrared, a spectral region interesting for gas sensing and pollution monitoring. Since the demonstration of the QCLs in 1994 in the InGaAs/InAlAs system grown on InP, the laser performance has been improved dramatically. For many applications there is a need for continuous tunable single mode sources, which can be realized by distributed feedback (DFB) lasers.

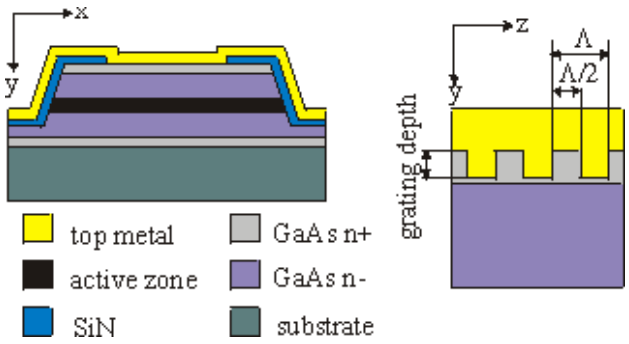

Fig. 7: Schematic cross sections of the DFB QCL and the grating region.

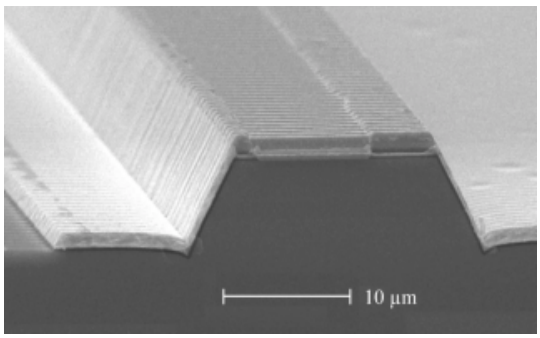

Fig. 8: Image of a fabricated device.

We fabricated distributed feedback quantum cascade lasers in the GaAs/AlGaAs material system, emitting at a wavelength of $\lambda = 10$ µm. The chosen laser design allows a simple fabrication technology without regrowth. The first order grating (grating period $\Lambda = 1.6$ µm) used for distributed feedback is etched into the surface of the upper cladding layer and covered with gold (Fig. 7 and Fig. 8). A deep etched ridge is used for lateral optical and electrical confinement. Vertical light confinement is achieved by a double plasmon enhanced optical waveguide. The active zone of our QCLs is based on intersubband transitions and consists of 30 periods of injector/active cell.

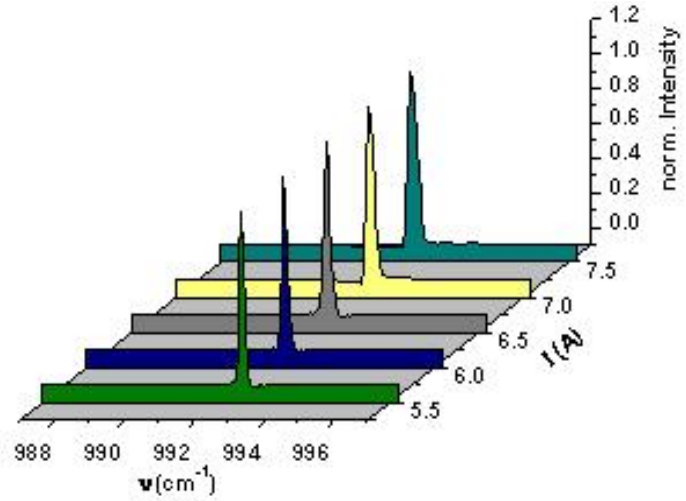

Fig. 9: Normalized emission spectra.

Single mode emission (Fig. 9) is observed with a linewidth smaller than $\Delta\nu = 0.2$ cm^{-1}, limited by the measurement setup. The emission wavenumber can be tuned continuously with the temperature at a rate of $d\nu/dT = 0.048$ cm^{-1}/K. We measured a coupling coefficient of $\kappa = 24$cm^{-1}, which is in good agreement with the numerical calculations based on a rigorous Floquet-Bloch theory.